Pharmaceutical Research, Vol. 26, No. 7, July 2009 (© 2009)
DOI: 10.1007/s11095-009-9886-2

Research Paper

Combination Chemotherapeutic Dry Powder Aerosols via Controlled Nanoparticle Agglomeration

Nashwa El-Gendy[1] and Cory Berkland[1,2,3,4]

Received December 23, 2008; accepted March 27, 2009; published online May 5, 2009

Purpose. To develop an aerosol system for efficient local lung delivery of chemotherapeutics where nanotechnology holds tremendous potential for developing more valuable cancer therapies. Concurrently, aerosolized chemotherapy is generating interest as a means to treat certain types of lung cancer more effectively with less systemic exposure to the compound.
Methods. Nanoparticles of the potent anticancer drug, paclitaxel, were controllably assembled to form low density microparticles directly after preparation of the nanoparticle suspension. The amino acid, L-leucine, was used as a colloid destabilizer to drive the assembly of paclitaxel nanoparticles. A combination chemotherapy aerosol was formed by assembling the paclitaxel nanoparticles in the presence of cisplatin in solution.
Results. Freeze-dried powders of the combination chemotherapy possessed desirable aerodynamic properties for inhalation. In addition, the dissolution rates of dried nanoparticle agglomerate formulations (~60% to 66% after 8 h) were significantly faster than that of micronized paclitaxel powder as received (~18% after 8 h). Interestingly, the presence of the water soluble cisplatin accelerated the dissolution of paclitaxel.
Conclusions. Nanoparticle agglomerates of paclitaxel alone or in combination with cisplatin may serve as effective chemotherapeutic dry powder aerosols to enable regional treatment of certain lung cancers.

KEY WORDS: cisplatin; combination chemotherapy; dry powder; nanoparticle agglomerates; paclitaxel.

INTRODUCTION

Lung cancer is the second most prevalent type of cancer and the most common cause of cancer-related death worldwide (1–3). Inefficient delivery of anticancer drugs to the disease site after intravenous or oral administration is a probable cause for the limited efficacy of some chemotherapeutics. Subsequently, the outcome for the treatment of lung cancer has not significantly progressed in recent history and the cure rate remains one of the lowest among all malignancies (4).

Currently, the most common application of aerosol therapy is regional drug delivery for airway and parenchyma lung diseases; however, there is also expanding interest in using the lung for systemic drug delivery (5). Dry powder inhalers (DPI) are emerging as a preferred drug delivery method compared to metered dose inhalers and nebulizers due to the improved stability of dry powders and the ease of use of the device (6,7). Inhalation is an attractive delivery route for chemotherapeutics as it offers several advantages over systemic and oral routes, including the probability of regional drug delivery to the lungs and airways. High local drug concentration may lower therapeutic doses, reduce systemic side effects, reduce the metabolic degradation of drugs in the liver, and offer noninvasive delivery (8,9).

Nanoparticle formulation of anticancer drugs has become an important research area in cancer therapy that may ultimately provide a way of sustained, controlled and targeted drug delivery to improve the therapeutic effect and reduce the side effects of the formulated drugs (10–12). For example, dissolution of poorly water soluble drug nanoparticles can be rapid and subsequently, drug bioavailability may be improved (13–15). However, the properties of nanoparticles can make them difficult to process into dry powders (16–19).

Aerosolized chemotherapy has to be precisely delivered at a therapeutic concentration to the target area to be effective (8). Delivery of pharmaceutical aerosols to the deep lung presents significant challenges to a formulator (20). Aerosol particle size is one of the vital determinants of aerosol dose and distribution in the lungs (21). To reach the peripheral airways and deposit in the alveolar region of the

Electronic supplementary material The online version of this article (doi:10.1007/s11095-009-9886-2) contains supplementary material, which is available to authorized users.

[1] Department of Pharmaceutical Chemistry, The University of Kansas, Lawrence, Kansas 66047, USA.
[2] Department of Chemical and Petroleum Engineering, The University of Kansas, Lawrence, Kansas 66047, USA.
[3] The University of Kansas, 2030 Becker Drive, Lawrence, Kansas 66047, USA.
[4] To whom correspondence should be addressed. (e-mail: berkland@ku.edu)

lung, aerosol particles need to be ~1–5 μm in aerodynamic diameter. Particles larger than 5 μm usually deposit in the oral cavity or upper airways, from which they are easily cleared. In contrast, particles smaller than 0.5 μm may be exhaled, since they settle very slowly (22). In addition, such nanoparticles can be highly cohesive due to the high surface area to mass ratio of the particulates. Cohesive systems pose a problem as uncontrolled agglomeration may lead to formulation variations and a decrease in dosing efficacy (18,23).

Recently, therapeutic interventions using combined chemotherapeutic drugs have emerged in cancer treatment as they have been proven to be more effective than a single drug (24–26). Combination chemotherapy remains the cornerstone of treatment for both limited-stage and extensive-stage small cell lung cancer (SCLC) (27,28). In the context of non-small cell lung cancer (NSCLC), drug combinations most frequently used for initial chemotherapy are cisplatin or carboplatin combined with other chemotherapeutic drugs such as paclitaxel (24). Higher response rates and a statistically significant improvement in survival were observed in a study of paclitaxel/cisplatin combination compared to many other cisplatin combinations. There was also a trend towards improved 1-year survival (29). Therefore, inhaled paclitaxel alone or in combination with cisplatin may be desirable.

Paclitaxel is an antineoplastic agent that works by inhibiting cellular growth through the promotion and stabilization of microtubule assembly by non-covalent interaction with tubulin, thereby blocking cell replication (30,31). It is a powerful anticancer drug with an established activity against a number of human, solid tumors and has become standard treatment as single agent or in combination chemotherapy for the management of advanced breast, ovarian and non-small-cell lung cancer (32). Paclitaxel possesses an extremely low aqueous solubility (<0.03 mg/mL) (33). Consequently, the formulation of paclitaxel has been a challenge, and many approaches have been tested or are under exploration. Significant advances in cancer treatment may be realized by the discovery and development of novel paclitaxel dosage forms with improved efficiency, reduced toxicity, and an expanded spectrum of activity (34). Cisplatin [*cis*-diamminedichloro platinum (II)] has been one of the most widely used and effective cytotoxic agents in the treatment of malignancies of lung, head and neck, testis, and ovarian cancers (35–37). Cisplatin is still the backbone of chemotherapy combinations in NSCLC, and several combinations of cisplatin-based chemotherapy are used in the current treatment of this disease (25).

A promising dry powder aerosol of paclitaxel as a single agent or in combination with cisplatin was formulated using an approach to controllably assemble paclitaxel nanoparticles into low-density microparticles. Paclitaxel nanoparticle suspensions were formulated using appropriate surfactants for pulmonary administration that control the size and surface charge of the prepared nanoparticles. The resulting colloidal suspensions were destabilized via ionic charge interactions using a suitable flocculating agent followed by lyophilizing the nanoparticle agglomerates into dry powder. In the case of the combined therapy formulation, an aqueous solution of cisplatin was injected into the paclitaxel nanoparticle suspension followed by addition of the agglomerating agent. These micron-sized agglomerates were easily aerosolized and exhibited enhanced dissolution. The powders reported here offer a novel formulation for localizing chemotherapy in the treatment of lung cancer.

MATERIALS AND METHODS

Materials

Paclitaxel (PX), cisplatin (CP), L-α-phosphatidylcholine (lecithin; Lec), cetyl alcohol (CA), L-leucine (Leu), polyvinylpyrrolidone (PVP K90, Mw ~ 36,000) and sodium chloride (NaCl) were purchased from Sigma Chemicals Co, St Louis, MO, USA. Pluronic F-127 (PL, Mw ~ 12,220) was purchased from BASF, The Chemical Company, Shakopee, MN, USA. Polyvinyl alcohol (PVA; Mw = 22,000, 88% hydrolyzed) was purchased from Acros Organics, New Jersey, NJ, USA. Potassium dihydrogen phosphate (KH_2PO_4), disodium hydrogen phosphate (Na_2HPO_4), acetone, ethanol, nitric acid and acetonitrile were purchased through Fisher Scientific, Fair Lawn, NJ, USA. Floatable dialysis membrane units (Regenerated Cellulose Membranes, manufactured from natural cellulose reconstituted from cotton linters, Mw cut-off = 10,000 Da) were obtained from Spectrum Laboratories Inc., Rancho Dominguez, CA, USA. A549 cells were obtained from the American Type Culture Collection (ATCC, Rockville, MD). The cell culture medium (Ham's F-12 Nutrient Mixture, Kaighn's modified with L-glutamine) was purchased through Fisher Scientific. Fetal bovine serum (FBS) was purchased from Hyclone, Logan, UT, USA. Penicillin–streptomycin was purchased from MB Biomedical, LLC, Winnipeg, MB, USA. Trypsin–EDTA was purchased through Gibco, Carlsbad, CA, USA. MTS reagent [tetrazolium compound; 3-(4,5-dimethylthiazol-2-yl)-5-(3-carboxymethoxyphenyl)-2-(4-sulfophenyl)-2H-tetrazolium, inner salt] was purchased from Promega, Madison, WI, USA. Double-distilled water was used throughout the study, provided by an EASYpure® RODI (Barnstead International, Model # D13321, Dubuque, Iowa, USA).

Fabrication of Paclitaxel Nanoparticles

Nanosuspensions were generated using a precipitation technique by slow injection of 2.5 mL acetone solution of paclitaxel, 0.1% *w/v*, in 25 mL distilled water at a rate of 1 mL/min under ultrasonication (probe-type sonicator, Fisher Scientific, Sonic Dismembrator) operating at an amplitude of 46%. Various surfactants were selected for the formulation of nanoparticles including hydrophobic (cetyl alcohol), hydrophilic (PL, PVA and PVP K90) and amphoteric (lecithin). The hydrophobic and amphoteric surfactants were added to the drug solution and the contents were sonicated in a bath-type sonicator (Branson 3510) for 30 min to allow complete solubilization of the drug and the surfactants. Hydrophilic surfactants were added to the aqueous phase. Surfactants were used individually or in combination as reported.

Characterization of the Prepared Nanoparticles

The particle size and zeta potential of the nanosuspensions were determined by dynamic light scattering (Brookhaven, ZetaPALS, Holtsville, NY, USA). Particle size was measured using distilled water while zeta potential measure-

ments were performed using 1 mM KCl solution. Triplicate measurements of all samples were performed.

Combination Chemotherapy of Paclitaxel Nanoparticles/Cisplatin Powder

The combined chemotherapeutic formulations were prepared by slow injection of 2.5 mL cisplatin aqueous solution to the paclitaxel nanosuspension (F1) during homogenization at 25,000 rpm. The two drugs were combined, at a ratio of 3:2 *w*/*w*, paclitaxel:cisplatin (29,32).

Agglomeration of Paclitaxel Nanoparticles and Combined Chemotherapy Formulation

Nanoparticle agglomerates were prepared by addition of L-leucine powder to the nanosuspensions followed by homogenization at 25,000 rpm for 30 s. The amount of L-leucine added was adjusted to a paclitaxel:leucine ratio equal to 1:1. The size of the nanoparticle agglomerates was measured in Isoton diluent using a Coulter Multisizer 3 (Beckman Coulter Inc., Miami, FL, USA) equipped with a 100 μm aperture after 3 h of incubation with the flocculating agent. The suspensions were kept overnight at room temperature to allow evaporation of acetone and then frozen at −80°C and transferred to a freeze dryer (Labconco, FreeZone 1, Kansas City, MO, USA). Drying lasted for 36 h to remove all appreciable water content. Lyophilized powder was stored at room temperature for further characterization.

Characterization of the Selected Nanoparticle Agglomerates

Determination of Particle Size Distribution

The particle size of the nanoparticle agglomerates immediately after flocculation as well as the resuspended lyophilized powder was measured using a Coulter Multisizer 3.

Angle of Repose and Bulk Density Measurements

The flow properties of the nanoparticle agglomerates were assessed by angle of repose measurement of the dried powders (38). The fixed-height cone method was used. A glass funnel with cut stem surface of 5 mm internal diameter was fixed at 2.5 cm height over a flat surface. The powders were allowed to flow gently through the funnel until a cone was formed and reached the funnel orifice. The flow of powder was then stopped and the average diameter of the formed cone (D) was measured. The angle of repose was calculated by the equation: $\tan\theta$=height/radius.

Furthermore, the bulk and tap densities were determined for the dried powders and compared with that of the paclitaxel powder as received. Ten milligrams of lyophilized powders were weighed and poured into a 10 mL graduated measuring cylinder. The bulk volume occupied (V_b) was recorded. The measuring cylinder was tapped until a constant value was obtained and the tap volume was recorded (V_t). The process was repeated at least three times and the average was taken in each case. The bulk (ρ_{bulk}) and tap (ρ_{tap}) densities of powders were calculated by dividing the weight by the corresponding bulk volume or tapped volume recorded. Carr's "percent compressibility" and Hausner ratio were calculated using the equation $\left(\left[\rho_{tap}-\rho_{bulk}\right]/\rho_{tap}\right)\times 100$) and ρ_{tap}/ρ_{bulk}, respectively. Angle of repose, Hausner ratio and Carr's index are considered indirect methods of quantifying powder flowability. The following ranges are indicative of good flow properties: 25–30° for angle of repose, <1.25 for Hausner ratio, 5–15% for Carr's index (38,39).

Measurement of Mass-median Aerodynamic Diameter

The aerodynamic size distributions of the agglomerate powders were measured directly from lyophilized powders by time-of-flight measurement using an Aerosizer LD (Amherst Instruments, Hadley, MA, USA) equipped with a 700 μm aperture operating at 6 psi.

The theoretical mass–mean aerodynamic diameter (d_{aero}) of the nanoparticle agglomerates was determined from the geometric particle size and tap density using the following relationship (40,41):

$$d_{aero}=d_{geo}\left[\frac{(\rho/\rho_{ref})^{0.5}}{\gamma}\right]$$

Where d_{geo}=geometric diameter, γ=shape factor (for a spherical particle, γ=1; for aerodynamic diameter calculations, the particles in this study were assumed to be spherical), ρ=particle bulk density and ρ_{ref}=water mass density (1 g/cm^3). Tapped density measurements underestimate particle bulk densities since the volume of particles measured includes the interstitial space between the particles. The true particle density, and the aerodynamic diameter of a given powder, is expected to be slightly larger than reported (42).

In Vitro Aerosolization Performance

Aerodynamic properties of the dry powders were investigated *in vitro* using a Tisch Ambient Cascade Impactor (Tisch Environmental, Inc., Village of Cleves, OH, USA). The study was carried out by applying ~10 mg dry powder manually into the orifice of the instrument operated at an air flow rate of ~30 L/min for 10 s to simulate an inspiration. Cut-off particle aerodynamic diameters of each stage of the impactor were: preseparator (10.00 μm), stage 0 (9.00 μm), stage 1 (5.8 μm), stage 2 (4.7 μm), stage 3 (3.3 μm), stage 4 (2.1 μm), stage 5 (1.1 μm), stage 6 (0.7 μm), stage 7 (0.4 μm) and filter (0 μm). Nanoparticle agglomerates deposited on each stage of the impactor were determined by measuring the difference in weight of filters placed on the stages. The percent emitted fraction (%EF) and fine particle fractions of the total dose (FPF_{TD}) were then calculated (42–44). The percent emitted fraction was determined from the following equation:

$$\%\ \text{Emitted fraction (\%EF)} = \frac{\text{Total particle mass collected from the stages of the impactor}}{\text{Total particle mass entered into the impactor}} \times 100$$

The fine particle fraction of the total dose (FPF_{TD}) was calculated as the percentage of aerosolized particles that

reached the lower seven stages of the impactor (corresponding to aerodynamic diameters below 5.8 μm), or the lower five stages (corresponding to aerodynamic diameters below 3.3 μm) according to the following equation (42):

$$\%\ \text{Fine particle fraction } (FPF_{TD}) = \frac{\text{Powder mass recovered from terminal stages of the impactor}}{\text{Total particle mass recovered in the impactor}} \times 100$$

Furthermore, the mass median aerodynamic diameter, MMAD, and geometric standard deviation, GSD, were obtained by a linear fit of the cumulative percent less-than the particle size range by weight plotted on a probability scale as a function of the logarithm of the effective cut-off diameter (45,46). GSD of the nanoparticle agglomerates was determined from the following equation:

$$GSD = \left(\frac{d_{84.13\%}}{d_{15.87\%}}\right)^{1/2}$$

where d_n is the diameter at the nth percentile of the cumulative distribution.

Concerning the dry powder of the combined chemotherapy, drug concentrations deposited on each stage of the impactor were determined. The powder deposited on each stage was collected after weighing and dissolved in 10 mL ethanol. The dispersion was sonicated in a bath-type sonicator (Branson 3510) for 1 h. Then the solution was centrifuged (Beckman, Avanti™) at ~15,000 rpm for 30 min and the amount of paclitaxel in the supernatant was determined using a reverse-phase HPLC method (12,47) while cisplatin content was detected by analyzing platinum metal in both supernatant and precipitate after dissolving the precipitate in 10 mL phosphate buffered saline (PBS, pH 7.4) using an atomic absorption spectrophotometer (Spectra AA 220G, Varian) (36,37,48).

Imaging of Particles by Transmission Electron Microscopy

Image data was used to corroborate the size of nanoparticles and nanoparticle agglomerates and to observe their morphological aspects. Transmission electron micrographs (TEM) were obtained for paclitaxel nanoparticles and nanoparticle agglomerates using a JEOL 1200 EXII transmission electron microscope. Initially, carbon-coated grids (Electron Microscopy Sciences) were floated on a droplet of the suspensions on a flexible plastic film (Parafilm), to permit the adsorption of the particles onto the grid. After this, the grid was blotted with a filter paper and air dried for 1 h.

Thermal Analysis

Nanoparticles and nanoparticle agglomerates were investigated by differential scanning calorimetry (DSC, Q100 Universal V4.3A TA instruments) and thermogravimetric analysis (TGA, Q50 Universal V4.3A TA instruments). For DSC analysis, a small portion (6–10 mg) of the lyophilized dry mass was sealed and placed in an aluminum pan and heated at a constant rate of 10°C/min over a temperature range of 25–300°C for paclitaxel powder as received, lecithin, L-leucine, nanoparticles and nanoparticle agglomerate formulation (F2). An inert atmosphere was maintained by purging with nitrogen at 50 mL/min. For TGA, samples weighing 5± 2 mg were scanned at a rate of 10°C/min with a nitrogen flow rate of 40 mL/min.

Determination of Process Yield and Paclitaxel Loading in Nanoparticle Agglomerates

Nanoparticle agglomerate dry powders were quantified and the yield was calculated for each formula using the following expression:

$$\%\ \text{Process yield} = \frac{\text{Recovered mass}}{\text{Mass entered into the experiment}} \times 100$$

Paclitaxel loading in the dry powders was assessed by dispersing one mg of the lyophilized powder in 10 mL ethanol. The dispersion was sonicated in a bath-type sonicator for 30 min. Then the solution was centrifuged at ~15,000 rpm for 30 min to remove insoluble ingredients and the amount of paclitaxel in the supernatant was determined using a reverse-phase HPLC method. On the other hand, cisplatin content in the combination formula was detected by analyzing platinum metal in both supernatant and residue after dissolving the residue in 10 mL PBS (pH 7.4) using the atomic absorption spectrophotometer. Drug loading was defined as follows (47,49):

$$\%\text{Loading} = \frac{\text{Recovered paclitaxel mass}}{\text{Total mass}} \times 100$$

Dissolution Studies

The dissolution of the prepared nanoparticles and nanoparticle agglomerates was determined under sink condition and compared with the dissolution characteristics of the drug powder as received. The dissolution of paclitaxel was carried out at 37±0.5°C in a 1 L beaker. Lyophilized powder (~10 mg) was dispersed in 10 mL PBS, pH 7.4 and was suspended into a floatable dialysis membrane unit (Mw cut-off=10,000 Da). The unit was allowed to float in 500 mL of PBS and the whole assembly was stirred at a constant speed (100 rpm) using a magnetic stirrer (Barnstead, Thermolyne MIRAK™). At predetermined time intervals for a total period of 8 h, serial samples (1 mL) of the medium were withdrawn from the dialysis bag and replaced with fresh medium. Then the samples were centrifuged for 30 min at ~13,000 rpm. The nanoparticle-free supernatant was removed and the residue was extracted with 1 mL of ethanol (12,49). The ethanol extract was analyzed for paclitaxel concentration using the reverse-phase HPLC method. In the case of the combined chemotherapy formula, the supernatant was analyzed for cisplatin concentration using the atomic absorption spectrophotometer. Studies were conducted in triplicate. Phosphate buffered saline (PBS, pH 7.4) was composed of 2.38 g Na_2HPO_4, 0.19 g KH_2PO_4 and 8 g NaCl.

Table I. Composition of Paclitaxel Formulations Used in the Studies

Formulation	Paclitaxel (% *w*/*v*)	Lecithin (% *w*/*v*)	PVP K90 (% *w*/*v*)	Cetyl alcohol (% *w*/*v*)
F1	0.1	0.02	0.01	
F2	0.1	0.02		
F3	0.1	0.02		0.01

HPLC Analysis of Paclitaxel

A reverse-phase HPLC method was used for quantifying paclitaxel samples ($n=3$). A Shimadzu HPLC system including a solvent delivery pump (Shimadzu LC-10AT), a controller (Shimadzu SCL-10A), an autoinjector (Shimadzu SIL-10AxL), and a UV detector (Shimadzu SPD-10A) was used in this study. The peak areas were integrated using Shimadzu Class VP (Version 4.3). A 4.6 mm×125 mm long Kromasil 100-5 C-8 column was used. During the assay, paclitaxel was eluted isocratically at a mobile phase flow rate of 0.9 mL/min and monitored with a UV detector operating at 228 nm. The mobile phase for the assay consisted of an acetonitrile and water mixture (50:50 *v*/*v*) (12,47). The run time for the assay was 20 min, and the retention time for paclitaxel was 10.7±0.1 min.

Atomic Absorption Spectroscopy for Cisplatin (AAS)

Cisplatin samples ($n=3$) were diluted 200-fold with 0.1% nitric acid for analysis. Analysis was performed on a Varian SpectrAA GTA-110 with graphite furnace and partition tubes. Samples (21 μL) were injected using the autosampler, followed by 19 μL of 0.1% nitric acid. Every ten samples were bracketed by calibration standards at 50, 75, and 150 ng/mL, and a quality control sample (50 or 75 ng/mL) every five samples. The furnace program was as follows: ramp 25 to 80°C, hold 2 s, ramp to 120°C, hold 10 s, ramp to 1,000°C, hold 5 s, ramp to 2,700°C, hold 2 s, cool to 25°C over 20 s. The graphite partition tube was cleaned every 500 injections samples by baking at 2,800°C for 7 s. Argon was used as the injection and carrier gas.

Cytotoxicity Assessment

The cytotoxicity of paclitaxel nanoparticle and nanoparticle agglomerate formulations was evaluated using the CellTiter 96® Aqueous Cell Proliferation Assay (Promega) and compared with paclitaxel powder as received, lecithin, PVP K90, L-leucine, physical mixtures of the ingredients used for the preparation of the selected formulas (F1 and F2) and blank nanoparticle agglomerates. In this experiment, A549 cells were cultured for 2 days. Then 8×10^4 A549 cells/well were seeded in 96-well microtiter plates and incubated for 24 h before adding the formulas. The tested chemicals were suspended in water and the A549 cells were incubated with serial dilutions of these chemicals (0.000625–5 mg/mL). At the end of the incubation period (24 h), 20 μL of MTS reagent solution was added to each well and incubated for 3 h at 37°C. The absorbance was measured at 490 nm using a microtiter plate reader (SpectraMax, M25, Molecular Devices Corp., Sunnyvale, CA, USA). The percentage of viable cells with all tested concentrations was calculated relative to untreated cells (50,51).

Table II. Physical Properties of Paclitaxel Nanoparticles (Values=Average±S.D.)

Formulation	Nanoparticle size (nm)	Zeta-potential (mV)	Polydispersity
F1[a]	299±10	25.1±0.7	0.04±0.03
F2[b]	339±14	24.7±1.5	0.18±0.1
F3[c]	359±8.0	22.4±1.0	0.31±0.1

[a] F1=0.1:0.02:0.01; PX:Lec:PVP K90
[b] F2=0.1:0.02; PX:Lec
[c] F3=0.1:0.02:0.01; PX:Lec:CA

RESULTS AND DISCUSSION

Paclitaxel Nanoparticle Fabrication

Precipitation methods are able to create nanoparticles of poorly water soluble drugs such as paclitaxel (52–54). Using this technique, nanoparticle suspensions were designed with different types and concentrations of surfactants, individually or in combination, as a means to control the particle size and surface charge of the prepared nanoparticles. Surfactants were chosen from a selection of excipients likely to be suitable for inhalation and proven to be safe for human use in certain concentrations (6).

Based on particle size and polydispersity measurements, the most successful surfactant combination and ratios for generating paclitaxel nanosuspension turned out to be the formulations; reported in Table I. These surfactant combinations yielded small paclitaxel particle size (298–358 nm). Formula, F1, was chosen for the combination with cisplatin as it showed smaller particle size and narrower size distribution with higher yield compared to the other formulas. A small change in zeta potential was observed with different types of surfactants and the values ranged from ~22–25 mV (Table II). The charged surface of the

Table III. Particle Size Characteristics of Paclitaxel Nanoparticle Agglomerates (Values=Average±S.D.)

Characteristics	Formulations		
	F1[a]	F2[b]	F1 Comb[c]
Geometric particle size (μm) of NA[d] before lyophilization	2.8±1	3.7±1	2.5±0.4
Geometric particle size (μm) of lyophilized NA[d]	4.8±1	5.4±2	5.9±3
$MMAD_A$[e] of lyophilized NA[d]	1.5±0.1	1.7±0.4	1.8±0.01
$MMAD_t$[f] of lyophilized NA[d]	1.1±1	1.2±1	1.5±0.1

[a] F1=0.1:0.02:0.01; PX:Lec:PVP K90
[b] F2=0.1:0.02; PX:Lec
[c] F1 Comb=3:2; PX:CP
[d] NA: nanoparticle agglomerates
[e] $MMAD_A$: mass median aerodynamic diameter obtained from Aerosizer
[f] $MMAD_t$: theoretical mass mean aerodynamic diameter calculated from density measurements

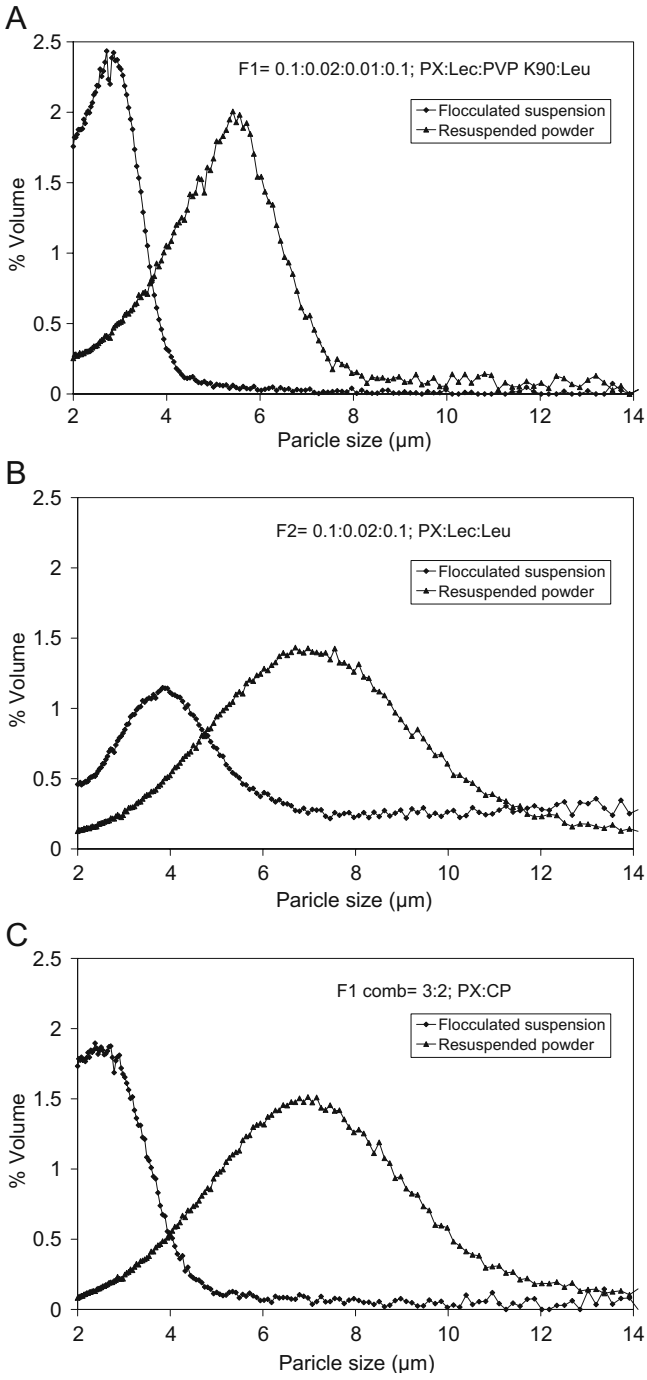

Fig. 1. The particle size distributions of paclitaxel nanoparticle agglomerates and F1 combination in suspension after flocculation and resuspended after lyophilization, for formulations **A** F1, **B** F2 and **C** F1 combination.

nanoparticles, provided by the surfactants, offered the potential for destabilizing this colloid via interaction with a flocculating agent to form nanoparticle agglomerates.

Agglomeration of Paclitaxel Nanoparticles

The mechanism to control nanoparticle agglomeration is mainly driven by leveraging the competitive processes of attraction (van der Waals force) and repulsion (electrostatic repulsive force or steric hindrance or both). If particles are mainly stabilized electrostatically, disruption of the electrostatic double layer surrounding the particles will result in the agglomeration of nanoparticles. The addition of flocculating agents has also been speculated to decrease the cohesion between particles (*e.g.* nanoparticle agglomerates). It is thought that these agents may interfere with weak bonding forces between small particles, such as van der Waals and Coulomb forces. They also may act as weak links or "chain

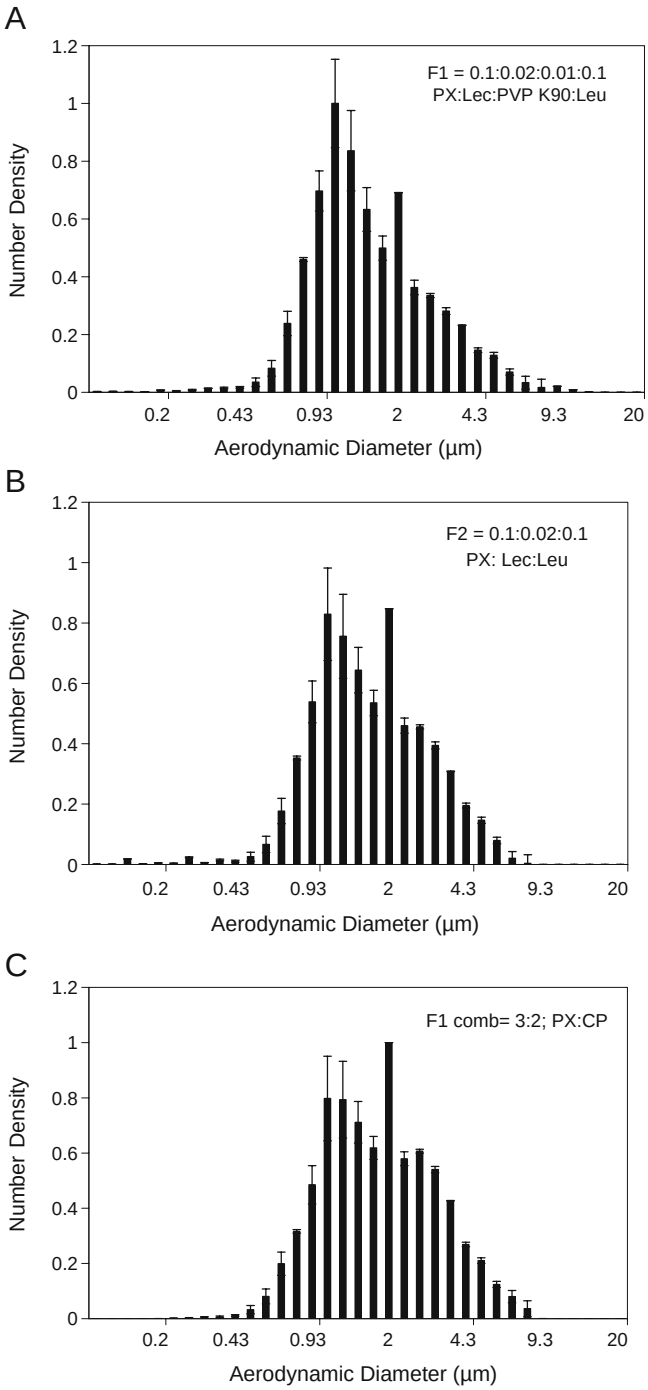

Fig. 2. Aerodynamic size distributions of paclitaxel nanoparticle agglomerates and F1 combination after lyophilization, for formulations **A** F1, **B** F2 and **C** F1 combination.

Table IV. Flowability Characteristics of Paclitaxel Nanoparticle Agglomerates (Values=Average±S.D.)

Formula no.	Angle of repose (θ)	Bulk density (g/cm^3)	Tapped density (g/cm^3)	Carr's index (Ci %)	Hausner ratio
Paclitaxel as received	27±1	0.2±0.1	0.3±0.01	19±0.03	1.3±0.04
Cisplatin as received	31±0.4	0.3±0.1	0.4±0.02	20±0.1	1.4±0.1
F1[a]	24±1	0.04±0.1	0.05±0.01	16±0.04	1.2±0.1
F2[b]	23±1	0.03±0.03	0.04±0.01	13±0.1	1.1±0.1
F1 Comb[c]	32±2	0.05±0.003	0.06±0.01	18±0.1	1.2±0.2

[a] F1=0.1:0.02:0.01; PX:Lec:PVP K90
[b] F2=0.1:0.02; PX:Lec
[c] F1 Comb=3:2; PX:CP

breakers" between the particles which are susceptible to disruption in the turbulent airstream created during inhalation (55,56).

Flocculation of paclitaxel nanoparticles and nanoparticles combined with cisplatin resulted in the formation of agglomerates ~1–5 μm. The geometric size distribution of the prepared nanoparticle agglomerates was measured in Isoton diluent using a Coulter Multisizer 3. The average size of two selected nanoparticle agglomerate formulations (F1 and F2) and the combination chemotherapy (F1 comb) ranged from ~2–4 μm (Table III). However, F3 showed very large agglomerates and a broad size distribution (~5–8 μm). This may be attributed to the surfactant mixture, which is an important determinate of the agglomeration of drug nanoparticles. Therefore, F3 was excluded from further characterization. The size distributions of resuspended lyophilized powders were slightly broader and the average particle size was increased to some extent when compared to the nanoparticle agglomerates in suspension prior to lyophilization (Table III and Fig. 1). This may be due to the deposition of nanoparticles on agglomerates during lyophilization or to cohesion between agglomerates as a result of drying (57). Furthermore, it was clear that the combination lyophilized powders had a broader distribution compared to the other two formulations (F1 and F2). This may have resulted from the agglomeration of powders of different particle sizes including paclitaxel nanoparticles and cisplatin powder, or from the uncontrolled formation of cisplatin-rich particles.

The aerodynamic diameter (d_{aero}) is regarded as an important physical parameter that predicts the site of aerosol deposition within the lungs (58). The aerodynamic diameter of the flocculated nanoparticles, measured by an Aerosizer LD, was found to be smaller than the geometric diameter and the aerodynamic size distribution was narrower than the geometric size distribution (Table III and Fig. 2). This reflects the low density of the nanoparticle agglomerates.

The flow characteristics of the selected nanoparticle agglomerates were also determined by calculating Angle of repose, Hausner ratio and Carr's index (Table IV). Nanoparticle agglomerates demonstrated improved and acceptable flow properties. Improvement in flowability may be partially explained by the reduced bulk and tap densities of the nanoparticle agglomerates compared to that of the drug powder as received. In addition, L-leucine has been reported to reduce surface energy in dry powders and may improve flowability in this case (59,60).

The theoretical mass–mean aerodynamic diameters (d_{aero}) of the nanoparticle agglomerates, determined from the geometric particle size and tap density were found to be 1.1, 1.2 and 1.5 μm for F1, F2 and F1 combination, respectively (Table III). Paclitaxel nanoparticle agglomerates with d_{aero} in this range may be expected to deposit primarily in the alveolar region of the lungs (58). Aerosizer results and theoretical MMAD calculations were confirmed by cascade impaction studies at an air flow rate of ~30 L/min (Fig. 3). Most nanoparticle agglomerates were deposited in stages 5–7 of the cascade impactor which was indicative of efficient aerosolization and a high fine particle fraction. However, F1 combination nanoparticle agglomerates exhibited some deposition on stages 0 and 1.

The aerosolization efficacy was represented by the percent emitted fraction (%EF), fine particle fraction of the total dose (FPF_{TD}), mass-median aerodynamic diameter (MMAD) and geometric standard deviation (GSD). The high emitted fraction of nanoparticle agglomerates obtained at the tested flow rate (~71–78%) suggested efficient aerosolization of the powder (Table V).

Cascade impaction data suggested that the anticipated total lung deposition (*i.e.* FPF_{TD} <5.8 μm) was about 95% and deep lung deposition (*i.e.* FPF_{TD}<3.3 μm) was about 80% for paclitaxel dry powder formulations, F1 and F2 (Table V). However, F1 combination dry powders exhibited an estimated total lung deposition of 79% and deep lung deposition of 71%, which were slightly lower than that found for the dry

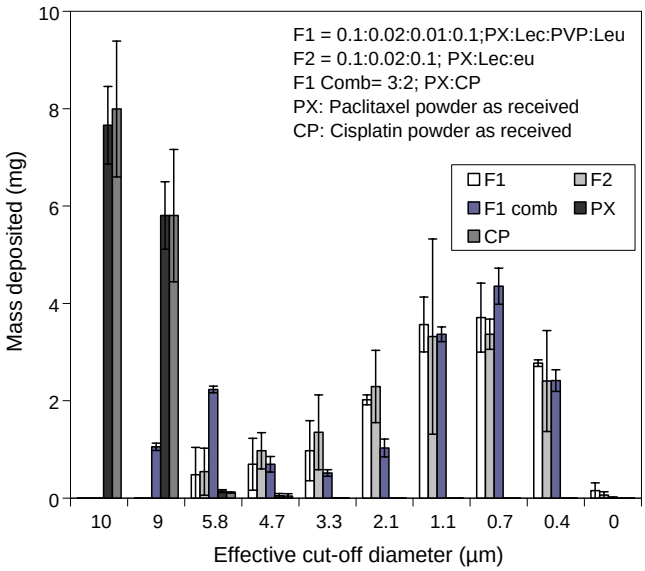

Fig. 3. The distribution of paclitaxel and cisplatin powder as received as well as nanoparticle agglomerate formulations deposited on the stages of a cascade impactor at a flow rate of ~30 L/min.

Table V. Cascade Impaction Results of Lyophilized Paclitaxel Nanoparticle Agglomerates (Values=Average±S.D.)

Characteristics of the lyophilized NA[d]			Formulations				
			F1[a]	F2[b]	F1 Comb[c]	Paclitaxel as received	Cisplatin as received
At flow rate of ~30 L/min	% EF[e]		72±5	72±15	78±1	68±6	70±1
	% FPF[f]	<5.7	96±3	95±4	79±1	0.4±0.3	0.3±0.4
		<3.3	84±3	80±5	71±1	0	0
	MMAD[g]		1.5±0.1	1.9±0.4	1.8±0.04	9.5±0.04	9.5±0.1
	GSD[h]		2.2±0.1	2.3±0.1	2.2±0.2	1.9±0.1	3.5±0.1

[a] F1=0.1:0.02:0.01; Px:Lec:PVP K90
[b] F2=0.1:0.02; Px:Lec
[c] F1 Comb=3:2; PX:CP
[d] NA: nanoparticle agglomerates
[e] % EF: percent emitted fraction
[f] FPF: fine particle fraction
[g] MMAD: mass median aerodynamic diameter obtained from cascade impactor
[h] GSD: geometric standard deviation

powders containing paclitaxel alone. All formulas offered the potential of high fine particle fraction suggesting excellent aerosol performance (61).

The mass–mean geometric size of nanoparticle agglomerates ranged between 4.8 and 5.9 μm with a GSD of ~2.3 μm (Table V). Typical GSD values for aerosol particles are between 1.3–3.0 (46). The mass-median aerodynamic diameter (MMAD) of the selected nanoparticle agglomerates, as calculated from the cascade impaction results (Table V) was found to be close to that obtained from the Aerosizer and the theoretical MMAD calculations (Table 3).

By chemically analyzing the powder of F1 comb that deposited on each stage of the cascade impactor, it was clear that the highest percent of paclitaxel and cisplatin was shown in stage 6 (42.8% and 39.5) followed by stage 5 (27.6% and 22.4) and then stage 7 (13.4 and 11.6), respectively (Fig. 4). However, cisplatin exhibited a slightly higher percent of powder in stages zero and one than paclitaxel. This was likely result of segregation of some larger cisplatin-rich particles during drying.

Particle Imaging

Electron microscopy was used to study the morphology of paclitaxel nanoparticles and nanoparticle agglomerate formulations. Transmission electron micrographs (TEM) of F1 nanoparticles illustrated slightly elongated nanoparticles with smooth surfaces and a particle size around 300 nm (Fig. 5A). TEM images of F1 nanoparticle agglomerates showed that the nanoparticles were flocculated into micron sized agglomerates of approximately 2–3 μm resembling bundles of elongated paclitaxel particles (Fig. 5B). A TEM image of the F1 combination showed the flocculation of paclitaxel nanoparticles after drying with cisplatin (Fig. 5C). The combination powders generally appeared slightly larger and rough particles (presumably cisplatin) appeared to be deposited on the rod-shaped paclitaxel particles.

Thermal Analysis (DSC and TGA)

The thermal properties of paclitaxel nanoparticles and nanoparticle agglomerates of formula F2 were investigated by differential scanning calorimetry (DSC) and thermogravimetric analysis (TGA). The DSC curve of paclitaxel powder as received exhibited a very small change in baseline around 60°C due to the presence of residual, probably absorbed or nonstructural water. The curve also showed an endothermic peak of melting at 220.7°C with an enthalpy change of 72.53 J/g just prior to an exothermic degradation peak (Table VI and Fig. 6) (62). For lecithin and L-leucine powders, there was a sharp melting endotherm at 168.2°C and 323.7°C, respectively. No paclitaxel melting peak was found in F2 nanoparticles. The curve also exhibited a small change in baseline ~60°C, probably due to the presence of absorbed or nonstructural water (47). Paclitaxel in the nanoparticle agglomerates also exhibited a small change in baseline at ~60°C and a shallow broad endothermic peak at the same position where the drug as received underwent a melting phenomenon upon heating; however, the characteristic peaks of the excipients were not apparent (Fig. 6). It was also clear that there was a significant increase in the heat of

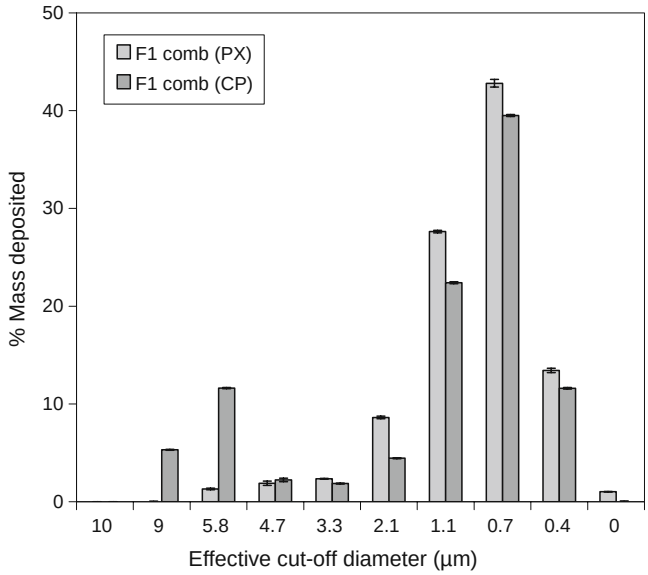

Fig. 4. The percent of paclitaxel and cisplatin in F1 combination nanoparticle agglomerate formulation deposited on the stages of a cascade impactor at a flow rate of ~30 L/min.

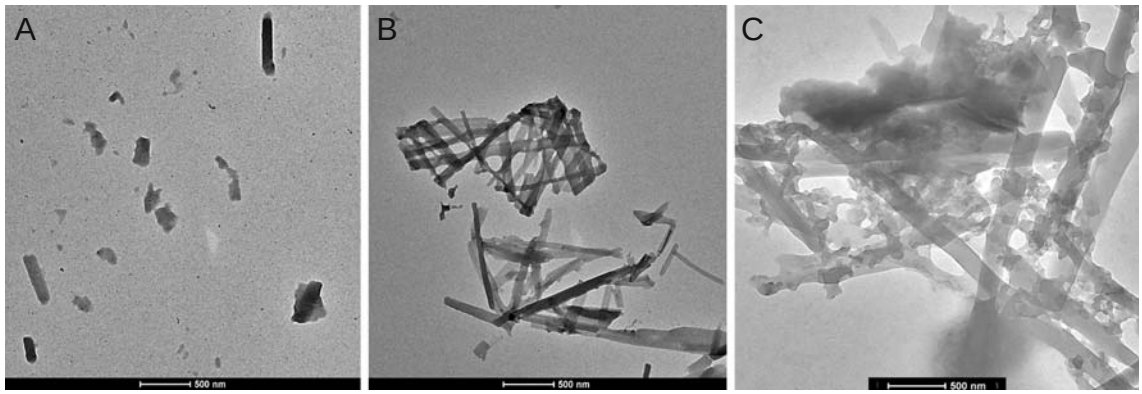

Fig. 5. Transmission electron micrographs of **A** F1 nanoparticles **B** F1 nanoparticle agglomerates and **C** F1 combination.

enthalpy compared to the pure drug. This may be indicative of some re-crystallization of the drug during the agglomeration process.

A systemic thermogravimetric analysis of paclitaxel powder as received revealed a 0.97% weight loss over the temperature range 10–200°C. The nanoparticles and nanoparticle agglomerates showed a higher weight loss of 2.45% and 2.48%, respectively (Fig. 7). The expected weight loss for paclitaxel dihydrate due to water evaporation is ~4.3%, which is approximately equivalent to two molecules of water per molecule of paclitaxel and the weight loss of amorphous paclitaxel was reported to be ~0.7% (63). In this case, the weight loss due to water evaporation (~2.4%) by TGA may reveal the presence of mixed morphologies of paclitaxel made of both the dihydrate and amorphous or "as received" crystalline forms.

Process Yield and Drug Loading

The process to agglomerate nanoparticles consistently achieved a high yield (~85–89%), which indicated efficient processing with minimum batch variability. The loading efficiency of paclitaxel in the prepared nanoparticle agglomerates (F1, F2 and F1 comb) was found to be ~85–93% (Table VII), and that of cisplatin in F1 comb was ~90%, thus demonstrating minimal loss of drug during powder preparation.

Table VI. DSC Peak Integrations for Paclitaxel, Lecithin and L-leucine Powders as Received as well as Paclitaxel Nanoparticles and Nanoparticle Agglomerates

Samples	Onset temp. (°C)	Peak temp. (°C)	Enthalpy (J/g)
Paclitaxel powder as received	211.5	220.7	72.5
Lecithin powder as received	167.7	168.2	31.6
L-leucine powder as received	298.7	323.7	1,041
F2[a] NP[b]	–	–	–
F2[a] NA[c]	211.4	222.7	266.2

[a] F2=0.1:0.02; Px:Lec
[b] NP: nanoparticles
[c] NA: nanoparticle agglomerates

Paclitaxel Nanoparticle and Nanoparticle Agglomerates Showed Improved Dissolution Rates

Dissolution of paclitaxel from nanoparticles and nanoparticle agglomerates (F1 and F2) into PBS was faster than that of the paclitaxel powder as received which achieved only ~18.1% dissolved drug after 8 h (Table VII and Fig. 8A, B). The cumulative percentage of the drug dissolved from nanoparticle agglomerates (Q_{8h}) was found to be slower than that of the nanoparticles. F1 nanoparticle and nanoparticle agglomerate formulations exhibited faster drug dissolution than F2 which may be due to the incorporation of the hydrophilic surfactant, PVP K90.

Paclitaxel dissolution from the F1 combination was faster than that of the F1 nanoparticle agglomerates and slightly faster than that of the prepared nanoparticles in the first 80 min followed by similar dissolution behavior. This may be due to the increase in the hydrophilicity of paclitaxel nanoparticle agglomerates as a result of the presence of the water soluble cisplatin powder integrated within the agglomerates (12). In addition, the slower dissolution behavior of paclitaxel nanoparticles compared to paclitaxel nanoparticle agglomerates in the F1 combination may be due to the aggregation of some nanoparticles in suspension after preparation.

The dissolution behavior of cisplatin from the agglomerated combination was also faster to some extent (~100% after ~80 min) than cisplatin powder as received which

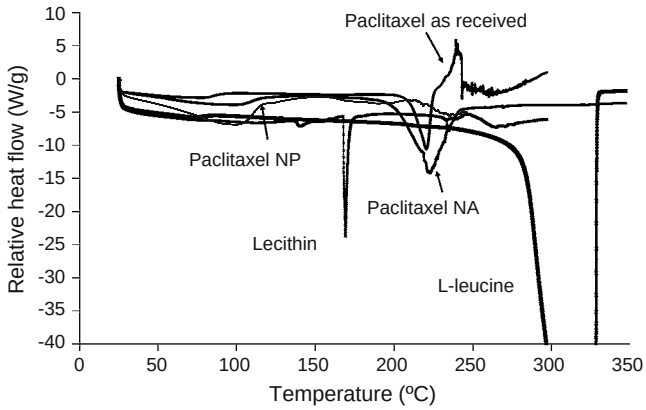

Fig. 6. Differential scanning calorimetry (DSC) thermograms for paclitaxel as received, nanoparticles (*NP*), nanoparticle agglomerates (*NA*), lecithin and L-leucine as received.

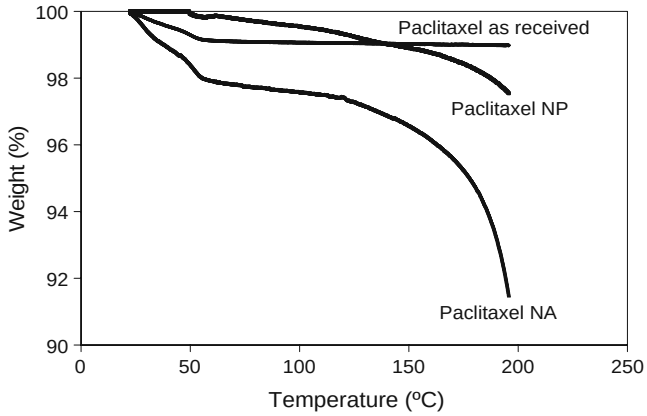

Fig. 7. Thermogravimetric analysis (TGA) for paclitaxel as received, nanoparticles (*NP*), and nanoparticle agglomerates (*NA*).

achieved ~100% after 2 h (Table VII and Fig. 8C). These findings may be due to the merging of cisplatin powder with paclitaxel nanoparticle agglomerates, which may result in a slight increase in the particle surface area thus enhancing the dissolution rate of cisplatin (14).

Linear regression analysis of the paclitaxel dissolution data concluded that the drug was released by the Higuchi diffusion mechanism in all cases. A two-way Analysis of Variance (ANOVA) was performed to determine the significance of differences in paclitaxel dissolution kinetics. Significant differences existed between nanoparticles, nanoparticle agglomerates and paclitaxel powder as received. This suggested a significant improvement ($P<0.05$) in the dissolution behavior of the nanoparticles and nanoparticle agglomerates when these were individually compared to the paclitaxel powder as received.

Measurement of Cytotoxicity

The cytotoxic effect of the different paclitaxel formulations was evaluated and compared to paclitaxel powder as received, lecithin, PVP K90, L-leucine, physical mixtures of F1 and F2 components and blank F1 and F2 nanoparticle agglomerates. It was clear that the excipients; lecithin, PVP K90 and leucine, did not show any notable cytotoxicity up to

Table VII. Yield, Loading and Dissolution Behavior of Paclitaxel Nanoparticle Agglomerates (Values=Average±S.D.)

Characteristics	Formulations		
	F1[a]	F2[b]	F1 Comb[c]
Process yield of lyophilized NA[d]	86±3%	90±3%	89±2%
% Drug loading of PX and CP in the lyophilized NA[d]	85±4%	86±9%	93±4% (PX) 90±5% (CP)
Q_{8h}[f] NP[e]	66±2%	61±13%	n/a
Q_{8h}[f] NA[d]	44±4%	40±3%	61±5% (PX) 100±2% (CP)

[a] F1=0.1:0.02:0.01; PX:Lec:PVP K90
[b] F2=0.1:0.02; PX:Lec
[c] F1 Comb=3:2; PX:CP
[d] NA: nanoparticle agglomerates
[e] NP: nanoparticles
[f] Q_{8h}: % Paclitaxel (PX) and cisplatin (CP) dissolved after 8 h

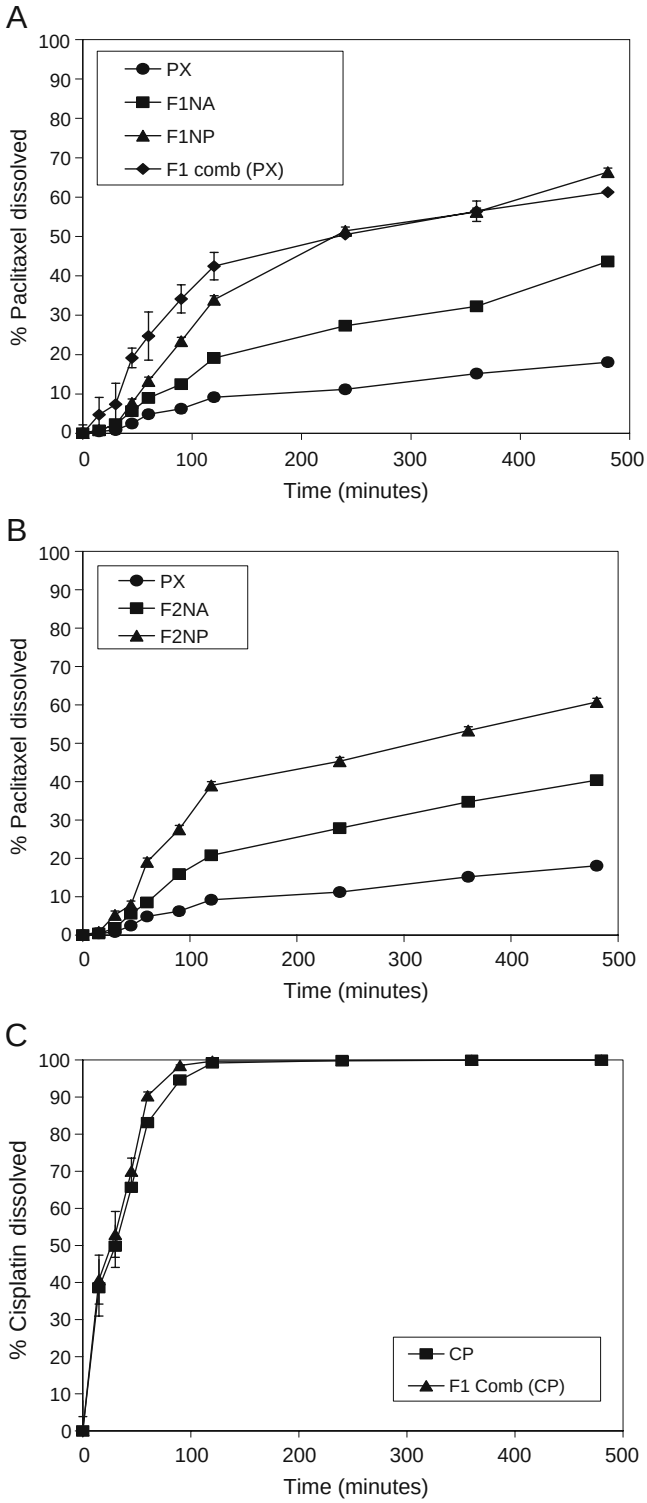

Fig. 8. Dissolution profiles of paclitaxel in PBS (pH 7.4) from **A**, **B** paclitaxel powder as received and two different nanoparticle formulations (*NP*), nanoparticle agglomerate formulations (*NA*) and F1 combination. **C** Dissolution profiles of cisplatin from cisplatin powder as received and from F1 combination.

5 mg/mL in A549 cells at the end of 12 h (Supplementary Fig. 1A, B). The IC_{50} values for all other samples occurred at concentrations higher than 1 mg/mL suggesting the safety of these formulations for preclinical study (31).

CONCLUSION

Methods of lung cancer treatment have not changed radically in recent history and the cure rate remains low. Single drug or combined chemotherapy regimens including cisplatin and paclitaxel may be recommended for non-small cell lung cancer and local delivery of these agents may ultimately improve the treatment of some types of lung cancer. In this work, paclitaxel nanosuspensions were successfully prepared via solvent precipitation in an aqueous solution. These colloids were destabilized using L-leucine to generate micron-sized agglomerates in a controlled fashion. Nanoparticles and nanoparticle agglomerates revealed enhanced dissolution kinetics when compared to the drugs as received. The nanoparticle agglomerate dry powders exhibited aerosol characteristics and size distributions appropriate for pulmonary drug delivery. Moreover, the development of paclitaxel nanoparticle agglomerates as a single agent or in combination with cisplatin demonstrated a desirable microstructure for efficient lung deposition and nanostructure for rapid dissolution of the poorly water soluble paclitaxel. In conclusion, this study offers an approach to localize combination lung cancer therapy using aerosolized nanoparticle powders.

ACKNOWLEDGEMENTS

We would like to acknowledge support for this work from the Coulter Foundation, the Higuchi Biosciences Center, and the Cystic Fibrosis Foundation as well as additional lab funding from the American Heart Association, the NIH (R03 AR054035, P20 RR016443 and T32 GM08359-11) and the Department of Defense. In addition, we acknowledge the support of the NSF (CHE 0719464). We also thank Prof. C. Russ Middaugh for the use of laboratory equipment and The Microscopy Lab for assistance with electron microscopy.

REFERENCES

1. Eramo A, Lotti F, Sette G, Pilozzi E, Biffoni M, Di Virgilio A, et al. Identification and expansion of the tumorigenic lung cancer stem cell population. Cell Death Differ 2008;15:504–14. doi:10.1038/sj.cdd.4402283.
2. Collins LG, Haines C, Perkel R, Enck RE. Lung cancer: diagnosis and management. Am Fam Phys 2007;75:56–63.
3. Hitzman CJ, Wattenberg LW, Wiedmann TS. Pharmacokinetics of 5-fluorouracil in the hamster following inhalation delivery of lipid-coated nanoparticles. J Pharm Sci 2006;95:1196–211. doi:10.1002/jps.20607.
4. Maillet A, Congy-Jolivet N, Le Guellec S, Vecellio L, Hamard S, Courty Y, *et al.* Aerodynamical, immunological and pharmacological properties of the anticancer antibody cetuximab following nebulization. Pharm Res 2008;25:1318–26. doi:10.1007/s11095-007-9481-3.
5. Scheuch G, Kohlhaeufl MJ, Brand P, Siekmeier R. Clinical perspectives on pulmonary systemic and macromolecular delivery. Adv Drug Deliv Rev 2006;58:996–1008. doi:10.1016/j.addr.2006.07.009.
6. Chougule MB, Padhi BK, Jinturkar KA, Misra A. Development of dry powder inhalers. Recent Pat Drug Deliv Formul 2007;1:11–21. doi:10.2174/187221107779814159.
7. Bosquillon C, Lombry C, Preat V, Vanbever R. Influence of formulation excipients and physical characteristics of inhalation dry powders on their aerosolization performance. J Control Release 2001;70:329–39. doi:10.1016/S0168-3659(00)00362-X.
8. Gagnadoux F, Hureaux J, Vecellio L, Urban T, Le Pape A, Valo I, *et al.* Aerosolized chemotherapy. J Aerosol Med Pulm Drug Deliv 2008;21:61–70. doi:10.1089/jamp.2007.0656.
9. Gagnadoux F, Pape AL, Lemarie E, Lerondel S, Valo I, Leblond V, *et al.* Aerosol delivery of chemotherapy in an orthotopic model of lung cancer. Eur Respir J 2005;26:657–61. doi:10.1183/09031936.05.00017305.
10. Praetorius NP, Mandal TK. Engineered nanoparticles in cancer therapy. Recent Pat Drug Deliv Formul 2007;1:37–51. doi:10.2174/187221107779814104.
11. Medina C, Santos-Martinez MJ, Radomski A, Corrigan OI, Radomski MW. Nanoparticles: pharmacological and toxicological significance. Br J Pharmacol 2007;150:552–8. doi:10.1038/sj.bjp.0707130.
12. Zhang Z, Feng SS. Nanoparticles of poly(lactide)/vitamin E TPGS copolymer for cancer chemotherapy: synthesis, formulation, characterization and *in vitro* drug release. Biomaterials 2006;27:262–70. doi:10.1016/j.biomaterials.2005.05.104.
13. Lindfors L, Skantze P, Skantze U, Westergren J, Olsson U. Amorphous drug nanosuspensions. 3. Particle dissolution and crystal growth. Langmuir 2007;23:9866–74. doi:10.1021/la700811b.
14. Matteucci ME, Hotze MA, Johnston KP, Williams RO 3rd. Drug nanoparticles by antisolvent precipitation: mixing energy *versus* surfactant stabilization. Langmuir 2006;22:8951–9. doi:10.1021/la061122t.
15. Rabinow BE. Nanosuspensions in drug delivery. Nat Rev Drug Discov 2004;3:785–96. doi:10.1038/nrd1494.
16. Tam JM, McConville JT, Williams RO 3rd, Johnston KP. Amorphous cyclosporin nanodispersions for enhanced pulmonary deposition and dissolution. J Pharm Sci 2008;97:4915–33. doi:10.1002/jps.21367.
17. Sepassi S, Goodwin DJ, Drake AF, Holland S, Leonard G, Martini L, *et al.* Effect of polymer molecular weight on the production of drug nanoparticles. J Pharm Sci 2007;96:2655–66. doi:10.1002/jps.20979.
18. Young PM, Chan HK, Chiou H, Edge S, Tee TH, Traini D. The influence of mechanical processing of dry powder inhaler carriers on drug aerosolization performance. J Pharm Sci 2007;96:1331–41. doi:10.1002/jps.20933.
19. Lindfors L, Forssen S, Skantze P, Skantze U, Zackrisson A, Olsson U. Amorphous drug nanosuspensions. 2. Experimental determination of bulk monomer concentrations. Langmuir 2006;22:911–6. doi:10.1021/la052367t.
20. Telkoand MJ, Hickey AJ. Dry powder inhaler formulation. Respir Care 2005;50:1209–27.
21. Labiris NR, Dolovich MB. Pulmonary drug delivery. Part I: physiological factors affecting therapeutic effectiveness of aerosolized medications. Br J Clin Pharmacol 2003;56:588–99. doi:10.1046/j.1365-2125.2003.01892.x.
22. Bhavna, Ahmad FJ, Khar RK, Sultana S, Bhatnagar A. Techniques to develop and characterize nanosized formulation for salbutamol sulfate. J Mater Sci Mater Med. 2008.
23. Chan H-K, Chew NYK. Novel alternative methods for the delivery of drugs for the treatment of asthma. Adv Drug Deliv Rev 2003;55:793–805. doi:10.1016/S0169-409X(03)00078-4.
24. N.C.C.N. Lung Cancer. Treatment Guidelines for patients. Version III:1–88 (2006).
25. Rosell R, Gatzemeier U, Betticher DC, Keppler U, Macha HN, Pirker R, *et al.* Phase III randomised trial comparing paclitaxel/carboplatin with paclitaxel/cisplatin in patients with advanced non-small-cell lung cancer: a cooperative multinational trial. Ann Oncol 2002;13:1539–49. doi:10.1093/annonc/mdf332.
26. Loehrer PJ Sr, Rynard S, Ansari R, Songer J, Pennington K, Einhorn L. Etoposide, ifosfamide, and cisplatin in extensive small cell lung cancer. Cancer 1992;69:669–73. doi:10.1002/1097-0142(19920201)69:3<669::AID-CNCR2820690312>3.0.CO;2-V.

27. Samelis GF, Ekmektzoglou KA, Xanthos T, Zografos GC. Small-cell lung cancer: an unusual therapeutic approach with more than 10-year overall survival. Case report and review of the literature. Tumori 2008;94:612–6.
28. Bhutani M, Pathak AK, Mohan A, Guleria R, Kochupillai V. Small cell lung cancer: an update on therapeutic aspects. Indian J Chest Dis Allied Sci 2006;48:49–57.
29. Earle CC, Coyle D, Evans WK. Cost-effectiveness analysis in oncology. Ann Oncol 1998;9:475–82. doi:10.1023/A:1008292128615.
30. Peltier S, Oger JM, Lagarce F, Couet W, Benoit JP. Enhanced oral paclitaxel bioavailability after administration of paclitaxel-loaded lipid nanocapsules. Pharm Res 2006;23:1243–50. doi:10.1007/s11095-006-0022-2.
31. Koziara JM, Lockman PR, Allen DD, Mumper RJ. Paclitaxel nanoparticles for the potential treatment of brain tumors. J Control Release 2004;99:259–69. doi:10.1016/j.jconrel.2004.07.006.
32. Yamamoto K, Kikuchi Y, Kudoh K, Hirata J, Kita T, Nagata I. Treatment with paclitaxel alone rather than combination with paclitaxel and cisplatin may be selective for cisplatin-resistant ovarian carcinoma. Jpn J Clin Oncol 2000;30:446–9. doi:10.1093/jjco/hyd116.
33. Singla AK, Garg A, Aggarwal D. Paclitaxel and its formulations. Int J Pharm 2002;235:179–92. doi:10.1016/S0378-5173(01)00986-3.
34. Liu Y, Chen GS, Chen Y, Cao DX, Ge ZQ, Yuan YJ. Inclusion complexes of paclitaxel and oligo(ethylenediamino) bridged bis (beta-cyclodextrin)s: solubilization and antitumor activity. Bioorg Med Chem 2004;12:5767–75. doi:10.1016/j.bmc.2004.08.040.
35. Ramachandran S, Quist AP, Kumar S, Lal R. Cisplatin nanoliposomes for cancer therapy: AFM and fluorescence imaging of cisplatin encapsulation, stability, cellular uptake, and toxicity. Langmuir 2006;22:8156–62. doi:10.1021/la0607499.
36. Uchino H, Matsumura Y, Negishi T, Koizumi F, Hayashi T, Honda T, *et al.* Cisplatin-incorporating polymeric micelles (NC-6004) can reduce nephrotoxicity and neurotoxicity of cisplatin in rats. Br J Cancer 2005;93:678–87. doi:10.1038/sj.bjc.6602772.
37. Nishiyama N, Okazaki S, Cabral H, Miyamoto M, Kato Y, Sugiyama Y, *et al.* Novel cisplatin-incorporated polymeric micelles can eradicate solid tumors in mice. Cancer Res 2003;63:8977–83.
38. Staniforth JN. Powder flow. In: Aulton ME, editor. Pharmaceutics: the science of dosage form design. London: Churchill Livingstone; 2002. p. 205–8.
39. Kumar V, Kothari SH, Banker GS. Compression, compaction, and disintegration properties of low crystallinity celluloses produced using different agitation rates during their regeneration from phosphoric acid solutions. AAPS PharmSciTech 2001;2:E7. doi:10.1208/pt020207.
40. Chow AHL, Tong HHY, Chattopadhyay P, Shekunov BY. Particle engineering for pulmonary drug delivery. Pharm Res 2007;24:411–37. doi:10.1007/s11095-006-9174-3.
41. Vanbever R, Mintzes JD, Wang J, Nice J, Chen D, Batycky R, *et al.* Formulation and physical characterization of large porous particles for inhalation. Pharm Res 1999;16:1735–42. doi:10.1023/A:1018910200420.
42. Fiegel J, Garcia-Contreras L, Thomas M, VerBerkmoes J, Elbert K, Hickey A, *et al.* Preparation and *in vivo* evaluation of a dry powder for inhalation of capreomycin. Pharm Res 2008;25:805–11. doi:10.1007/s11095-007-9381-6.
43. Yang ZY, Le Y, Hu TT, Shen Z, Chen JF, Yun J. Production of ultrafine sumatriptan succinate particles for pulmonary delivery. Pharm Res 2008;25:2012–8. doi:10.1007/s11095-008-9586-3.
44. Lechuga-Ballesteros D, Charan C, Stults CL, Stevenson CL, Miller DP, Vehring R, *et al.* Trileucine improves aerosol performance and stability of spray-dried powders for inhalation. J Pharm Sci 2008;97:287–302. doi:10.1002/jps.21078.
45. Pham S, Wiedmann TS. Note: dissolution of aerosol particles of budesonide in Survanta, a model lung surfactant. J Pharm Sci 2001;90:98–104. doi:10.1002/1520-6017(200101)90:1<98::AID-JPS11>3.0.CO;2-5.
46. Vanbever R, Ben-Jebria A, Mintzes JD, Langer R, Edwards DA. Sustained release of insulin from insoluble inhaled particles. Drug Dev Res 1999;48:178–85. doi:10.1002/(SICI)1098-2299(199912)48:4<178::AID-DDR5>3.0.CO;2-I.
47. Hu Y, Xie J, Tong YW, Wang CH. Effect of PEG conformation and particle size on the cellular uptake efficiency of nanoparticles with the HepG2 cells. J Control Release 2007;118:7–17. doi:10.1016/j.jconrel.2006.11.028.
48. Avgoustakis K, Beletsi A, Panagi Z, Klepetsanis P, Karydas AG, Ithakissios DS. PLGA-mPEG nanoparticles of cisplatin: *in vitro* nanoparticle degradation, *in vitro* drug release and *in vivo* drug residence in blood properties. J Control Release 2002;79:123–35. doi:10.1016/S0168-3659(01)00530-2.
49. Lu Z, Yeh TK, Tsai M, Au JL, Wientjes MG. Paclitaxel-loaded gelatin nanoparticles for intravesical bladder cancer therapy. Clin Cancer Res 2004;10:7677–84. doi:10.1158/1078-0432.CCR-04-1443.
50. Soundara Manickam D, Bisht HS, Wan L, Mao G, Oupicky D. Influence of TAT-peptide polymerization on properties and transfection activity of TAT/DNA polyplexes. J Control Release 2005;102:293–306. doi:10.1016/j.jconrel.2004.09.018.
51. Bandi N, Kompella UB. Budesonide reduces multidrug resistance-associated protein 1 expression in an airway epithelial cell line (Calu-1). Eur J Pharmacol 2002;437:9–17. doi:10.1016/S0014-2999(02)01267-0.
52. Matteucci ME, Brettmann BK, Rogers TL, Elder EJ, Williams RO 3rd, Johnston KP. Design of potent amorphous drug nanoparticles for rapid generation of highly supersaturated media. Mol Pharm 2007;4:782–93. doi:10.1021/mp0700211.
53. Bilati U, Allemann E, Doelker E. Development of a nanoprecipitation method intended for the entrapment of hydrophilic drugs into nanoparticles. Eur J Pharm Sci 2005;24:67–75. doi:10.1016/j.ejps.2004.09.011.
54. Govender T, Stolnik S, Garnett MC, Illum L, Davis SS. PLGA nanoparticles prepared by nanoprecipitation: drug loading and release studies of a water soluble drug. J Control Release 1999;57:171–85. doi:10.1016/S0168-3659(98)00116-3.
55. Kumar PV, Jain NK. Suppression of agglomeration of ciprofloxacin-loaded human serum albumin nanoparticles. AAPS PharmSciTech 2007;8:17. doi:10.1208/pt0801017.
56. Shi LJ, Berkland C. pH-Triggered dispersion of nanoparticle clusters. Adv Mater 2006;18:2315–9. doi:10.1002/adma.200600610.
57. Shi L, Plumley CJ, Berkland C. Biodegradable nanoparticle flocculates for dry powder aerosol formulation. Langmuir 2007;23:10897–901. doi:10.1021/la7020098.
58. Fiegel J, Fu J, Hanes J. Poly(ether-anhydride) dry powder aerosols for sustained drug delivery in the lungs. J Control Release 2004;96:411–23. doi:10.1016/j.jconrel.2004.02.018.
59. Shur J, Nevell TG, Ewen RJ, Price R, Smith A, Barbu E, *et al.* Cospray-dried unfractionated heparin with L-leucine as a dry powder inhaler mucolytic for cystic fibrosis therapy. J Pharm Sci 2008;97:4857–68. doi:10.1002/jps.21362.
60. Young PM, Cocconi D, Colombo P, Bettini R, Price R, Steele DF, *et al.* Characterization of a surface modified dry powder inhalation carrier prepared by "particle smoothing". J Pharm Pharmacol 2002;54:1339–44. doi:10.1211/002235702760345400.
61. Chew NY, Shekunov BY, Tong HH, Chow AH, Savage C, Wu J, *et al.* Effect of amino acids on the dispersion of disodium cromoglycate powders. J Pharm Sci 2005;94:2289–300. doi:10.1002/jps.20426.
62. Liggins RT, Hunter WL, Burt HM. Solid-state characterization of paclitaxel. J Pharm Sci 1997;86:1458–63. doi:10.1021/js9605226.
63. Gi U-S, Min B, Lee JH, Kim J-H. Preparation and characterization of paclitaxel from plant cell culture. Korean J Chem Eng 2004;21:816–20. doi:10.1007/BF02705526.